A gene network model accounting for development and evolution of mammalian teeth

Isaac Salazar-Ciudad*†‡§ and Jukka Jernvall‡§

*Complex Systems Research Group, Department of Physics and Nuclear Engineering, Polytechnic University of Catalonia, North Campus, Modul B5, 08034 Barcelona, Spain; †Department of Genetics, University of Barcelona, Diagonal 645, 08028 Barcelona, Spain; and ‡Developmental Biology Program, Institute of Biotechnology, University of Helsinki, P.O. Box 56, FIN-00014 Helsinki, Finland

Edited by David B. Wake, University of California, Berkeley, CA, and approved April 23, 2002 (received for review February 6, 2002)

Generation of morphological diversity remains a challenge for evolutionary biologists because it is unclear how an ultimately finite number of genes involved in initial pattern formation integrates with morphogenesis. Ideally, models used to search for the simplest developmental principles on how genes produce form should account for both developmental process and evolutionary change. Here we present a model reproducing the morphology of mammalian teeth by integrating experimental data on gene interactions and growth into a morphodynamic mechanism in which developing morphology has a causal role in patterning. The model predicts the course of tooth-shape development in different mammalian species and also reproduces key transitions in evolution. Furthermore, we reproduce the known expression patterns of several genes involved in tooth development and their dynamics over developmental time. Large morphological effects frequently can be achieved by small changes, according to this model, and similar morphologies can be produced by different changes. This finding may be consistent with why predicting the morphological outcomes of molecular experiments is challenging. Nevertheless, models incorporating morphology and gene activity show promise for linking genotypes to phenotypes.

Basic principles that may link genotype to phenotype can be examined by integrating molecular and cellular data into models (1, 2). Such models can be tested most convincingly by using both comparative neontological and paleontological data. Here we test the mechanistic relevance of known genetic data on tooth development and the plausibility that simple developmental principles may suffice for producing dental diversity.

Evolutionary diversity of mammalian radiations is best documented by the diversity in shape of individual tooth crowns, which are also well suited for disentangling how genes produce form. A substantial knowledge of basic gene interactions shows that an iterative signaling between the tooth epithelial and mesenchymal tissues is required for correct pattern formation and morphogenesis. Mediation of this process during the formation of tooth crowns occurs through a limited number of epithelial signaling centers, the enamel knots (3). The knots express genes common to other signaling centers involved in the formation of organs such as the limb (4, 5), feathers (6, 7), and brain (8, 9). In addition, the morphogenesis of teeth is largely unaffected by that of adjacent organs, making it easier to model the genetic basis of shape.

As a starting point, the model includes a set of identical epithelial cells lying above a set of identical mesenchymal cells. These cells lack any internal mechanisms that require an external coordinate system or a combinatorial code to provide unique positional information for individual cusps. This implementation fits the empirical data where no cusp-specific genes have been identified (3, 10). All of the cells can respond to two diffusible signaling molecules: an activator and an inhibitor, which affect growth of the tooth germ inversely (Fig. 1 *A* and *B*). The activator is an inducer of the nonproliferative epithelial knot, hence, inducer of cellular differentiation. The inhibitor, instead, represses knot differentiation and promotes growth. These dynamics follow the cell proliferation patterns found in developing teeth, and the model produces concentration peaks of both inhibitor and activator analogous to the gene expression patterns *in vivo* (Fig. 1*C*). Currently, over 50 genes have been documented to be expressed in the knots (http://bite-it.helsinki.fi/). Of those, 12 are signaling molecules belonging to the *Bmp*, *Fgf*, *Shh*, and *Wnt* gene families. They are expressed in nested patterns around the knots and their expression domains predict future cusp patterns (11). Established candidate molecules for activators include bone morphogenetic proteins (BMPs), which induce differentiation markers in the dental epithelia, associated with the cessation of mitosis in the knot (12, 13). Putative inhibitors include fibroblast growth factors (FGFs) and SHH, which stimulate growth and survival of dental epithelia, mesenchyme, or both (13–15), and of which at least FGFs induce an antagonist of BMPs (16). Our model differs from classic reaction-diffusion models, which incorporate growth (17–19), by using the spatial distribution of molecules that affect, and are in turn affected by, growth directly. In other words, in this model pattern formation and morphogenesis are mutually linked, a mechanism that we call here morphodynamic. Additionally, tooth growth (10, 11, 20–23) is biased along the bucco-lingual and anterio-posterior axes, and these biases are implemented as parameters in the model. BMPs expressed in the mesenchyme have been implicated as a source of these biases *in vivo* (12). Because we were interested in the most parsimonious principle capable of producing real shapes, we excluded variables such as cell shape and extracellular matrix from the model.

Model and Methods

Morphodynamic Model. The model depicts tooth development from the cap stage to the early bell stage (the primary enamel knot is the first knot in the model, reviewed in ref. 3). During the cap stage, a tooth crown begins to develop after the initial ingrowth of the epithelium into the underlying mesenchyme. Although most of the cusps are developing during the early bell stage, tooth mineralization has not yet begun. The epithelial growth rate is as a constant (R_e) intrinsic to the cells, minus the activator concentration. Initially, all epithelial cells secrete activator at an intrinsic rate (k_3) and also in response to the local activator concentration. Next, in areas where the local activator concentration exceeds a set threshold, the epithelial cells differentiate irreversibly into nondividing knot cells. These knot cells also secrete inhibitor at a rate equal to the local activator concentration. This inhibitor counteracts activator secretion and enhances growth of the mesenchyme depending on its concentration (the use of terms *activator* and *inhibitor* refer to the way these molecules interact). While the growing epithelium between knots folds into the mesenchyme leaving the knots isolated in the tips of the forming cusps, mesenchymal growth produces localized lateral expansion affecting cusp sharpness

This paper was submitted directly (Track II) to the PNAS office.

§To whom reprint requests should be addressed. E-mail: isalazar@mappi.helsinki.fi or jvakudaret@aol.com.

 www.pnas.org/cgi/doi/10.1073/pnas.132069499

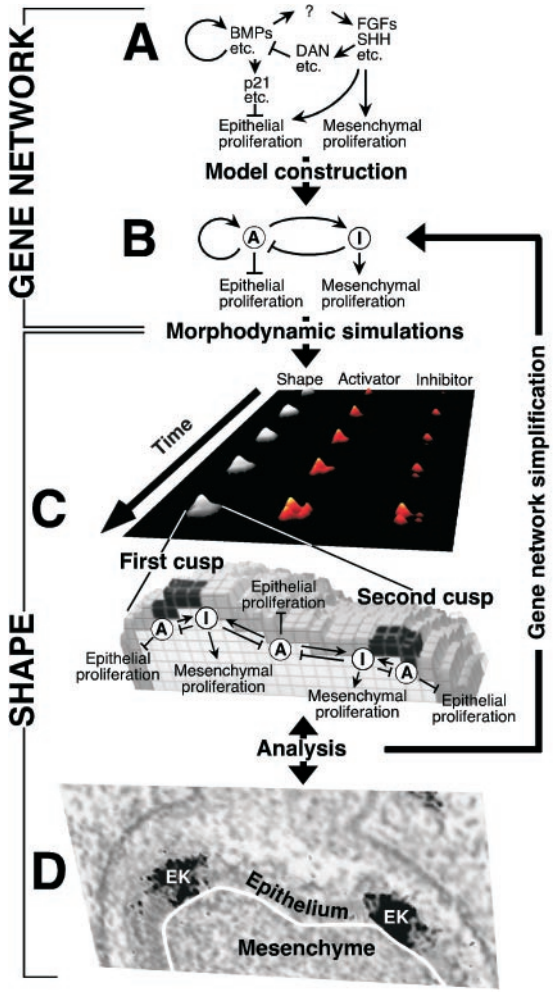

Fig. 1. Basic principles of the modeling approach and the morphodynamic model on tooth development. (*A*) The starting point of the model is an empirically derived simplified gene network based on both experimental and spatiotemporal gene expression data (putative gene groupings from teeth only, molecular effects are often context-dependent). (*B*) The final gene network after further simplification based on simulations and analyses. (*C*) To examine whether a gene network is sufficient in approximating tooth-shape development, the model produces three-dimensional shapes and distributions of activator and inhibitor concentrations peaks. (*D*) The simulated shapes are analyzed by comparing them to empirical data on developing tooth shapes. The simulations depict growth of the inner enamel epithelium above the dental mesenchyme separated by the basement membrane (white line in *D*). In actual teeth, the cells of the inner enamel epithelium differentiate into enamel-forming ameloblasts and the mesenchymal cells below differentiate into dentine-forming odontoblasts. In an erupting tooth the mesenchyme (papilla) forms the tooth pulp whereas the inner enamel epithelium and the overlying epithelial stellate reticulum are degraded, exposing enamel surface. The first cusp forms when epithelial cells differentiate into nondividing enamel knot cells (EK, *Fgf4* expression in black in *D*). This change happens in the model when activator ''A'' concentration reaches a set threshold. Knot cells secrete inhibitor ''I'', which counteracts the secretion of activator, thus also inhibiting the formation of the second cusp immediately adjacent to the first cusp (*C Lower*). In addition, unlike in classic reaction-diffusion models, activator and inhibitor modulate tissue growth, making developing shape itself have a causal role in the placement of new knots. For example, formation of the second cusp also depends on the relative sharpness of cusps, because sharpness modifies the volume of mesenchymal tissue into which molecules dilute.

(22, 23). The sharpness of cusps influences the effective distance at which new knots can form, because sharpness modifies the three-dimensional volume of mesenchymal tissue into which activator and inhibitor diffuse. Furthermore, cusp sharpness and growth of tooth borders influence the shape of the knots, which in turn affect the spatial distribution of new knots (Fig. 1*D*). Thus, knot formation always depends on previous morphology and not only on the spatial distribution of activator and inhibitor.

Model Implementation. The dynamics we consider take place in a portion of the inner dental epithelium and the dental mesenchyme that it encloses (Fig. 1*D*). Diffusion takes place inside the three-dimensional space (subdivided into a three-dimensional grid of boxes) of the growing tooth. The system can be visualized as a set of contiguous columns of cells in which cells that are in contact with the overlying stellate reticulum are epithelial and the rest are mesenchymal. The system has zero-flux boundary conditions in the epithelium (diffusion is not allowed) and open boundary conditions in the mesenchyme [molecules exit the system through the borders (24)]. Specifically, the inner enamel epithelium is in contact with the stellate reticulum in its apical side, (Fig. 1*D*) where diffusion is impeded, compared with that of its basal side, where the epithelium is in contact with basement membrane and mesenchyme (where diffusion is allowed) (25). The mesenchyme is surrounded by the epithelium (where diffusion is allowed), except in the ventral border containing the nondental mesenchyme (where diffusion is allowed). The rate of activator secretion in nonknot epithelial cells is

$$\frac{\partial A}{\partial t} = \frac{k_1[A]}{k_2[I] + 1} + k_3 + D_A\nabla^2[A], \qquad [1]$$

where $D_A\nabla^2 A$ is the diffusion term, and D_A is the diffusion coefficient of the activator. The k_1 and k_2 constants can be related to biochemical aspects as the affinity of each molecule for its receptor or to the amplification produced by its chain of signal transduction. The rate of inhibitor secretion by knot cells is

$$\frac{\partial I}{\partial t} = [A] + D_I\nabla^2[I], \qquad [2]$$

where $D_I\nabla^2 I$ is the diffusion term, and D_I is the diffusion coefficient of the inhibitor. Epithelial growth is implemented by making epithelia to increase its depth into the mesenchyme. When a single epithelial cell shifts ventrally one cell length into the mesenchyme, it displaces ventrally all of the underlying cells in that column, thus mimicking the downgrowth of valleys along with the retention of the crown base. Epithelial growth rate is $R_e - A$ and at least zero. The mesenchymal growth occurs mainly in the direction offering less resistance (away from turgid stellate reticulum). Visible expansion is thus lateral, and the force producing the expansion by a column of mesenchymal cells was calculated as the sum of the concentration of inhibitor in all of the cells of the column multiplied by a constant (R_m) that reflects the sensitivity of cells to the growth effect of the inhibitor. Specifically, the lateral force of cells in a column i is distributed into four nearest-neighboring columns (the anterior, posterior, buccal, and lingual columns) by the following rules: (*i*) force distribution is restricted to columns shorter than column i. (*ii*) The resistance ($1/Sj$) of each neighboring column shorter than column i is determined by the total number of cells in the cumulative in a given direction (for example, all of the posterior columns next to the column i). This reads

$$S_j = 1 \Big/ \left(\sum_{k=0}^{k=n(i,j)} \sum_{l=0}^{l=m(k)} 1 \right), \qquad [3]$$

where j can be any of the four directions (anterior, posterior, buccal, and lingual), $n(i,j)$ is the number of columns between column i and the border of the tooth in the direction j, and $m(k)$

EVOLUTION

is the number of cells in column k. Note that $n(i,j)$ and $m(k)$ depend on tooth shape at each time point and are not external functions or fixed parameters. (*iii*) The force of column i is distributed to its neighbors in inverse proportion to their resistance. This relation is defined as

$$R_j(i) = D_j R_m \sum_{k=0}^{k=m(i)} [I]_{ik}, \quad [4]$$

where $D_j = S_j/(S_p + S_a + S_b + S_l)$ for $j \in [p,a,b,l]$.

$R_j(i)$ is the rate of growth of column i in direction j. $[I]_{ik}$ is the concentration of the inhibitor in cell k in column i, and R_m is the rate constant of mesenchymal growth. S_j is the inverse of the resistance, and $(S_p + S_a + S_b + S_l)$ is the overall inverse of the resistance in all directions. The lateral expansion is mimicked by adding new cells when lateral force on a cell exceeds a unit corresponding to a cell size in a given direction. For a column that is not in the border of the tooth, the neighboring column of cells increases its height by one unit and a new cell is added at the bottom of the column, and for a column in the border of the tooth a new cell is added to extend the perimeter. All of the new cells appearing are considered epithelial if they are in contact with the stellate reticulum. Lateral growth is biased by increasing the lateral force on cells in the perimeters of the tooth. There is a bias in the posterior (B_p), anterior (B_a), buccal (B_b), and lingual (B_l) direction. For cells in the border j thus read

$$R_j(i) = D_j R_m \sum_{k=0}^{k=m(i)} [I]_{ik} + B_j \text{ for } j \in [p, a, b, l]. \quad [5]$$

We present only the results using the most parsimonious gene network (inhibitor affecting directly only mesenchyme growth, Fig. 1*B*); equivalent results are obtained if we include the effect of inhibitor on epithelium growth. Also, the exact kinetics by which activator and inhibitor affect each other can be varied and the mouse and vole shapes can still be produced by changing the parameters. The model was programmed in XBASIC (http://www.xbasic.org/) and is available with the code from the authors (http://biocenter.helsinki.fi/bi/craniofacial/Jernvall.htm).

Simulations and Empirical Data. The shape coordinates and activator and inhibitor concentrations for each time point (each simulation starts from four epithelial and mesenchymal cells and runs generally to 7,000 iterations, sampled approximately every 1,000 iterations) were plotted with the Geographic Information Systems (GIS) DIMPLE package (http://www.process.com.au/) and analyzed similarly to the observed teeth. The empirical GIS data on developing mouse and vole teeth (11) depict and the model simulates the early stages of morphogenesis, before dentine, enamel, and root formation. Therefore, only cuspal areas of predicted and observed shapes are illustrated, thus excluding more lateral and ventral aspects of teeth. For further details, see ref. 11. Other simulated tooth shapes were compared with examples in the literature and in our three-dimensional database. Note that comparisons with fully formed teeth, such as with fossils, are only indicative because the model does not simulate mineralization.

Results and Discussion

Because the model incorporates gene interactions and growth without an implicit code for cusp position or size, the initial set of cells contains no direct blueprint of the final patterns (Fig. 1). Therefore, to test how well the morphodynamic model approximates the actual process of tooth development, we explored the ability of the model to reproduce the distinct morphologies of the first lower molars of mouse (*Mus musculus*) and vole (*Microtus rossiaemeridionalis*). We chose mouse and vole molars because they are the first species in which detailed reconstructions of the three-dimensional morphology of various intermediate stages have been coupled with the patterns of expression of relevant genes. Such data have been attained by using GIS that have allowed quantification of gene expression patterns and three-dimensional morphology (11). Based on these analyses, we explored whether vole and mouse molars can be produced by simple changes in model parameters affecting growth, signaling, and directional bias.

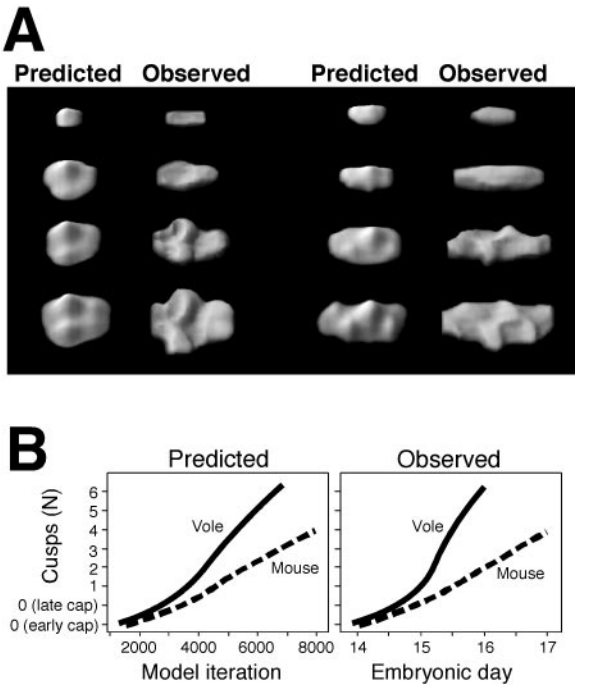

Fig. 2. The model predicts the course of development. (*A*) Predicted and observed development of mouse (*Left*) and vole (*Right*) first lower molar topography. The model reproduces the parallel and diagonal cusp configurations of mouse and vole, respectively. The illustrated predictions of vole differ from mouse by increase in the effect of inhibitors on activators and decrease in buccal bias in growth, and increase in anterior bias in growth. The shared parameter values for the illustrated mouse and vole predictions are $k_1 = 1.5$; $k_3 = 0\ 001$; $D_A = 0.3$; $D_I = 0.4$; $R_e = 0.0005722$; $R_m = 0.000465$; $B_p = 0.000756$; $B_b = 0.000240$. In the mouse and vole predictions, k_2, B_a, and B_l are 111, 0.0004508, and 0.0009932, and 78, 0.001020, and 0.000615, respectively. Anterior side is toward the left and the buccal side is toward the top. The advanced mouse and vole teeth are approximately 400 and 600 μm in length, respectively. (*B*) The simulations approximate the observed temporal spacing between developmental stages in the slow- and fast-growing mouse and vole molar, respectively.

Our model successfully reproduces not only the species specific crown morphologies, but also the morphology of all of the intermediate stages (Fig. 2*A*), including the correct temporal spacing between the stages (Fig. 2*B*). In addition, the activator and inhibitor concentration gradients (Fig. 1*C*) successfully reproduced the patterns of expression of known genes (Fig. 3*A*). Because the model reproduces the *course* of development of both mouse and vole shapes with associated gene expression patterns, it may predict the general process of tooth development. Compared with gene activity data *in vivo*, the model correctly predicts the nested patterns around the knots, activation of enamel knots in relation to folding of the epithelium, and the sequence of knot formation (Fig. 3*B*). The mouse and vole predictions were attained by choosing parameters that differ only slightly, thus evolution of disparate morphologies may not require extensive modification of the genome (Fig. 2*A*). Specifically, change from the diagonal cusp configuration of vole teeth to the parallel cusp configuration of mouse teeth required but a small increase in the bias of lingual growth (B_l) and stronger inhibition of activator by inhibitor (k_2), resulting in a spatial shift in knot formation similar

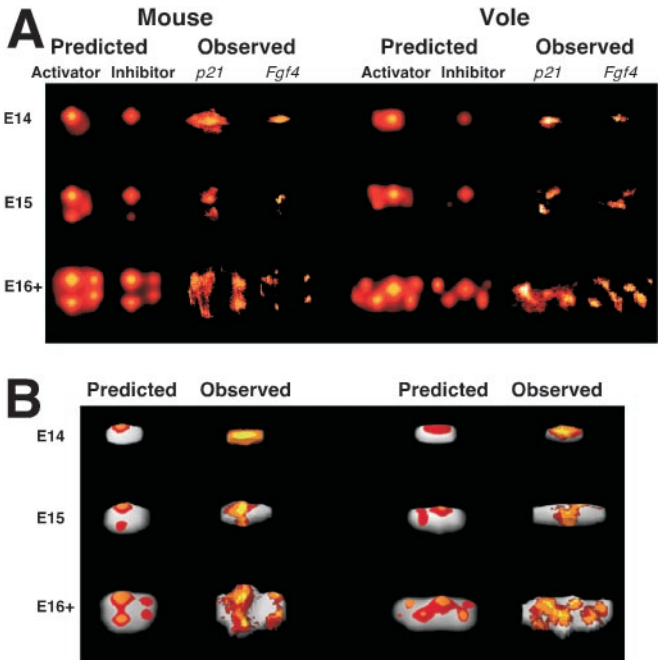

Fig. 3. The model predicts gene expression patterns in mouse (*Left*) and vole (*Right*). (*A*) The concentration peaks of activator and inhibitor (in lighter color) accurately predict the gene expression domains detected with *in situ* preparations (viewed from above). Note how the domains of high activator concentration match the expression of cyclin-dependent kinase inhibitor *p21* (target of Bmp signaling), expressed in differentiating epithelial cells, and how the domains of high inhibitor concentration match the expression of growth-stimulating fibroblast growth factor 4 (*Fgf4*), expressed inside the knots. (*B*) The activator and inhibitor concentration peaks predict the observed nested gene coexpression patterns among genes of different signaling families. On predicted shapes, the coexpression patterns of activator and inhibitor (in orange) inside the activator domain (in red) resemble the observed coexpression patterns where *Fgf4*, *Shh*, *Lef1*, and *p21* (in yellow) mark the cores of the enamel knots, surrounded by areas lacking *Fgf4* (in orange) and *Fgf4* + *Lef1* expressions (in red). Anterior side is toward the left and buccal side is toward the top; ages are in embryonic days.

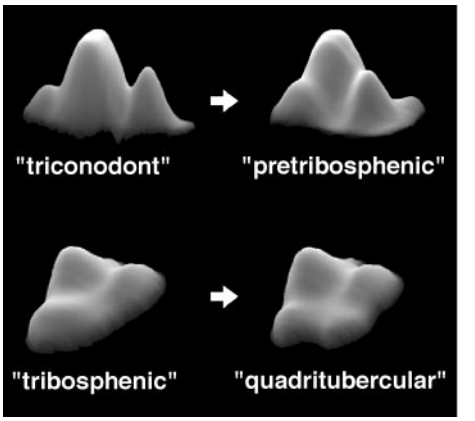

Fig. 4. Major transitions in mammalian molar evolution require small changes in the model parameters. The top pair show modeled triconodont and pretribosphenic shapes of lower molar. The pretribosphenic has been derived from the triconodont shape by adjusting parameters R_e and B_l. The bottom pair shows the modeled evolution of the hypocone (as the fourth cusp in the quadritubercular tooth) on the tribosphenic upper molars. The hypocone has evolved at least 20 times among mammalian lineages, and at least two different parameter changes ($k_2 = 109$ or $B_l = 0.000757$) can independently produce the hypocone in the model. The parameter values for the illustrated triconodont tooth are $k_1 = 1.5$; $k_2 = 110$; $k_3 = 0.001$; $D_A = 0.3$; $D_l = 0.4$; $R_e = 0.00095$; $R_m = 0.000465$; $B_a = 0.00045$; $B_p = 0.0007$; $B_l = 0.00015$; $B_b = 0.0001$, and the same for the pretribosphenic tooth except for $R_e = 0.00090$ and $B_l = 0.00056$. The tribosphenic parameters are $k_1 = 1.5$; $k_2 = 110$; $k_3 = 0.001$; $D_A = 0.3$; $D_l = 0.4$; $R_e = 0.0005722$; $R_m = 0.000465$; $B_a = 0.00024$; $B_p = 0.000955$; $B_l = 0.000756$; $B_b = 0.000442$, and the same for the quadritubercular tooth except for $k_2 = 109$. Obliquely lingual views; anterior side is toward the left.

to that found *in vivo* (ref. 11; Fig. 3). An increase in the anterior growth bias (B_a) produces the accelerated growth and greater number of cusps in the anterior part of a vole tooth (11).

The use of our model to predict the course of gene activity patterns raises questions about the roles of genes involved in tooth development. Although several growth factors expressed in the knot may affect growth (3, 13–15), our results uncover the minimal gene network that reproduces the real-world patterns. To this end, the model provides a framework for interpreting the roles of individual genes by identifying functional interactions between signaling molecules and growth. For example, molecules identified as inhibitors of knots (fibroblast growth factors, SHH) may be hypothesized to have somewhat analogous effects on patterning. Considering the shift in cusp positions between mouse and vole, the model indicates that at least one of the inhibitor molecules should counteract enamel knot differentiation more strongly in the mouse than in the vole teeth. The large number of expressed genes in developing teeth may be needed to mediate the basic gene network interactions in individual molecular cascades (e.g., ref. 16) or affect the basic parameters of the network to fine-tune and buffer development. We therefore propose that although gene networks regulating development seem highly complex (26), the underlying principles of the network organization may be relatively simple (27).

In addition to predicting the course of tooth shape development, a large spectrum of tooth shapes can be produced by modifying only a few model parameters (Fig. 4). Evolutionary patterns of mammalian molar tooth shape are diverse with complex cusp patterns evolving in many mammalian lineages. We suggest that the intricate gene network-morphology relationship described here may have allowed molar teeth to attain high diversity with only a few small genetic changes and without requiring prepatterns for different morphologies (Fig. 4). The model is not stochastic; hence, the same set of parameters always produces the same shape. Population level variation (28–30) can be hypothesized to arise from variation in parameters (or environmental modification of the action of the parameters).

Compared with the evolution of diverse molar tooth shapes across species, the same parameters may have been altered during the evolutionary origin of different tooth identities, such as incisor and molar classes. Differential expression of transcription factors has been implicated in determining different tooth identities (31–34). We suggest that such transcription factors may act by affecting some of the parameters of the morphodynamic model, for example the intrinsic rate of growth of the epithelia (R_e) or the rate of secretion of activator by the epithelia (k_1 or k_3). Also, we were able to obtain the results with a model where the first knot, corresponding to the primary enamel knot *in vivo* (3, 10, 11), was functionally similar to the later-forming knots. It remains a possibility that putative transcription factors determining tooth identities may alter tooth shape along the jaw by altering, for example, available tissue size for the primary enamel knot.

The evolutionary versatility of the model is an indication that although tooth morphology is effectively produced by genes, predicting the effects of small genetic changes on morphology becomes very complex, especially in the absence of a causal model predicting the outcome of such changes. We propose that this morphodynamic mechanism may be applicable to other complex morphological structures in which the positioning and

shape of signaling centers are affected by both the effects of emitted signals on cellular behaviors producing shape (morphogenesis) and the effects of the emitted signals on the expression of molecular signals in other cells (pattern formation). Examples of this may be seen in the face, brain, limbs, feathers, and various branching organs. Another evolutionary implication of the morphodynamic mechanism is that similar or identical morphologies can be attained for different combinations of the model parameters (Fig. 4). Therefore, although this may contribute to the frequent parallel and convergent evolution of tooth cusps (35) and substantiates inferences stemming from recent phylogenetic studies (36–38), genetic changes can differ in the evolution of similar tooth shapes. This result is also consistent with the general finding that the same phenotypic effects can be found in mutations of diverse molecular nature (39–43). In conclusion, the ability of our model to account for both developmental process and evolutionary change suggests that both mathematical models on, and accurate reconstruction of, three-dimensional morphologies and gene expression patterns (44) may be necessary for the linking of genotype to phenotype. In other words, shape during development matters.

We thank M. Fortelius, J. P. Hunter, H.-S. Jung, S. Keränen, S. A. Newman, S. T. Pochron, P. D. Polly, M. M. Smith, R. V. Solé, I. Thesleff, K. M. Weiss, and P. C. Wright for discussions and advice on this work. This work was supported by Academy of Finland Grant 48704 and by a grant from the Generalitat de Catalunya.

1. Gilbert, S. F. & Sarkar, S. (2000) *Dev. Dyn.* **219,** 1–9.
2. Salazar-Ciudad, I., Newman, S. A. & Solé, R. V. (2001) *Evol. Dev.* **3,** 84–94.
3. Jernvall, J. & Thesleff, I. (2000) *Mech. Dev.* **92,** 19–29.
4. Niswander, L., Jeffrey, S., Martin, G. R. & Tickle, C. (1994) *Nature (London)* **371,** 609–612.
5. Tickle, C. (2000) *Int. J. Dev. Biol.* **44,** 101–108.
6. Jung, H.-S., Francis-West, P. H., Widelitz, R. B., Jiang, T.-X., Ting-Berreth, S., Tickle, C., Wolpert, L. & Chuong, C.-M. (1998) *Dev. Biol.* **196,** 11–23.
7. Jiang, T., Jung, H.-S., Widelitz, R. B. & Chuong, C. (1999) *Development (Cambridge, U.K.)* **126,** 4997–5009.
8. Echelard, Y., Epstein, D. J., St-Jacques, B., Shen, L., Mohler, J., McMahon, J. A. & McMahon, A. (1993) *Cell* **75,** 1417–1430.
9. Agarwala, S., Sanders, T. A. & Ragsdale, C. W. (2001) *Science* **291,** 2147–2150.
10. Keränen, S. V. E., Åberg, T., Kettunen, P., Thesleff, I. & Jernvall, J. (1998) *Dev. Genes Evol.* **208,** 477–486.
11. Jernvall, J., Keränen, S. V. E. & Thesleff, I. (2000) *Proc. Natl. Acad. Sci. USA* **97,** 14444–14448.
12. Åberg, T., Wozney, J. & Thesleff, I. (1997) *Dev. Dyn.* **210,** 383–396.
13. Jernvall, J., Åberg, T., Kettunen, P., Keränen, S. & Thesleff, I. (1998) *Development (Cambridge, U.K.)* **125,** 161–169.
14. Kettunen, P., Laurikkala, J., Itäranta, P., Vainio, S., Itoh, N. & Thesleff, I. (2000) *Dev. Dyn.* **219,** 322–332.
15. Dassule, H. R., Lewis, P., Bei, M., Maas, R. & McMahon, A. P. (2000) *Development (Cambridge, U.K.)* **127,** 4775–4785.
16. Mandler, M. & Neubüser, A. (2001) *Dev. Biol.* **240,** 548–559.
17. Maini, P. K., Myerscough, M. R., Winters, K. H. & Murray, J. D. (1991) *Bull. Math. Biol.* **53,** 701–719.
18. Kondo, S. & Asai, R. (1995) *Nature (London)* **376,** 765–768.
19. Varea, C., Aragón, J. L. & Barrio, R. A. (1997) *Phys. Rev. E* **56,** 1250–1253.
20. Gaunt, W. A. (1961) *Acta Anat.* **45,** 219–251.
21. Marshall, P. M. & Butler, P. M. (1966) *Arch. Oral Biol.* **11,** 949–965.
22. Butler, P. M. (1967) *Arch. Oral Biol.* **12,** 983–992.
23. Popowics, T. E. (1998) *J. Morph.* **237,** 69–90.
24. Crick, F. (1970) *Nature (London)* **225,** 420–422.
25. Gritli-Linde, A., Lewis, P., McMahon, A. P. & Linde, A. (2001) *Dev. Biol.* **236,** 364–386.
26. Davidson, E. H., Rast, J. P., Oliveri, P., Ransick, A., Calestani, C., Yuh, C.-H., Minokawa, T., Amore, G., Hinman, V., Arenas-Mena, C., *et al.* (2002) *Science* **295,** 1669–1678.
27. Salazar-Ciudad, I., Garcia Fernandez, J. & Solé, R. V. (2000) *J. Theor. Biol.* **205,** 587–603.
28. Polly, P. D. (1998) *Paleobiology* **24,** 409–429.
29. Jernvall, J. (2000) *Proc. Natl. Acad. Sci. USA* **97,** 2641–2645.
30. Polly, P. D. (2001) *Genetica* **112,** 339–357.
31. Tucker, A. S., Matthews, K. L. & Sharpe, P. (1998) *Science* **82,** 1136–1138.
32. Zhao, Z., Weiss, K. M. & Stock, D. W. (2000) in *Development, Function and Evolution of Teeth*, eds. Teaford, M., Smith, M. M. & Ferguson, M. (Cambridge Univ. Press, Cambridge, U.K.), pp. 152–172.
33. Stock, D. W. (2001) *Philos. Trans. R. Soc. London B* **356,** 1633–1653.
34. McCollum, M. A. & Sharpe, P. T. (2001) *BioEssays* **23,** 481–493.
35. Hunter, J. P. & Jernvall, J. (1995) *Proc. Natl. Acad. Sci. USA* **92,** 10718–10722.
36. Naylor, G. J. P. & Adams, D. C. (2001) *Syst. Biol.* **50,** 444–453.
37. Gingerich, P. D., Haq, M., Zalmout, I. S., Khan, I. H. & Malkani, M. S. (2001) *Science* **293,** 2239–2242.
38. Thewissen, J. G. M., Williams, E. M., Ro, L. J. & Hussain, S. T. (2001) *Nature (London)* **413,** 277–281.
39. Alberch, P. (1980) *Am. Zool.* **20,** 653–667.
40. Horder, T. J. (1989) in *Complex Organismal Functions: Integration and Evolution in Vertebrates, Dahlem Konferenzen*, eds. Wake, D. W. & Roth, G. (Wiley, Chichester, U.K.), pp. 294–360.
41. Nijhout, H. F. (1991) *The Development and Evolution of Butterfly Wing Patterns* (Smithsonian Institution Press, Washington, DC).
42. Smith, K. K. & Schneider, R. A. (1998) *BioEssays* **20,** 245–255.
43. Weiss, K. M. & Fullerton, S. M. (2000) *Theor. Popul. Biol.* **57,** 187–195.
44. Streicher, J., Donat, M. A., Strauss, B., Sporle, R., Schughart, K. & Muller, G. B. (2000) *Nat. Genet.* **25,** 147–152.